

**ORIGINAL ARTICLE**

---

# A Comparison of Bone Marrow and Cord Blood Mesenchymal Stem Cells for Cartilage Self-Assembly

Jamie L. White, BA,<sup>1</sup> Naomi J. Walker, BA,<sup>2</sup> Jerry C. Hu, PhD,<sup>3</sup>  
Dori L. Borjesson, DVM, MPVM, PhD,<sup>2,4</sup> and Kyriacos A. Athanasiou, PhD, PE<sup>3</sup>

Joint injury is a common cause of premature retirement for the human and equine athlete alike. Implantation of engineered cartilage offers the potential to increase the success rate of surgical intervention and hasten recovery times. Mesenchymal stem cells (MSCs) are a particularly attractive cell source for cartilage engineering. While bone marrow-derived MSCs (BM-MSCs) have been most extensively characterized for musculoskeletal tissue engineering, studies suggest that cord blood MSCs (CB-MSCs) may elicit a more robust chondrogenic phenotype. The objective of this study was to determine a superior equine MSC source for cartilage engineering. MSCs derived from bone marrow or cord blood were stimulated to undergo chondrogenesis through aggregate redifferentiation and used to generate cartilage through the self-assembling process. The resulting neocartilage produced from either BM-MSCs or CB-MSCs was compared by measuring mechanical, biochemical, and histological properties. We found that while BM constructs possessed higher tensile properties and collagen content, CB constructs had superior compressive properties comparable to that of native tissue and higher GAG content. Moreover, CB constructs had alkaline phosphatase activity, collagen type X, and collagen type II on par with native tissue suggesting a more hyaline cartilage-like phenotype. In conclusion, while both BM-MSCs and CB-MSCs were able to form neocartilage, CB-MSCs resulted in tissue more closely resembling native equine articular cartilage as determined by a quantitative functionality index. Therefore, CB-MSCs are deemed a superior source for the purpose of articular cartilage self-assembly.

**Keywords:** cartilage, tissue engineering, mesenchymal stem cells, MSCs, equine

## Introduction

**J**OINT INJURY, DUE to either traumatic injury or a chronic degenerative process, leads to premature retirement for many athletes.<sup>1–3</sup> In particular, joint injury is an especially devastating and all-too-common occurrence for equine athletes. A study examining specific causes of morbidity in over 100,000 horses from 1997 to 2000 found joints to be the most commonly affected body system in this population.<sup>4</sup> As in humans and many other species, articular cartilage in horses does not readily regenerate and often results in the formation of mechanically inferior fibrocartilage rather than normal hyaline cartilage.<sup>5,6</sup> Large defects (>9 mm) fail to heal without intervention.<sup>7,8</sup> If joint

injury is treated in its early stages, surgical intervention can facilitate healing and help prevent joint degeneration; however, the success of this approach is limited by many factors such as age of the animal, as well as location and chronicity of the defect.<sup>9</sup> Engineering cartilage implants hold potential to increase the success rate of surgical intervention and hasten recovery times.

Cartilage tissue engineering for joint surface repair seeks to recapitulate the organized extracellular matrix of hyaline cartilage. Self-assembly is a scaffold-free approach to cartilage engineering in which chondrogenic cells are densely seeded in nonadherent culture and stimulated to generate extracellular matrix using medium supplementation.<sup>10</sup> After 4 weeks in culture, self-assembled chondrogenic cells

---

<sup>1</sup>Department of Pathology, Microbiology and Immunology, Integrative Pathobiology Graduate Group, University of California, Davis, Davis, California.

<sup>2</sup>Department of Pathology, Microbiology and Immunology, University of California, Davis, Davis, California.

<sup>3</sup>Department of Biomedical Engineering, Henry Samueli School of Engineering, University of California, Irvine, Irvine, California.

<sup>4</sup>School of Veterinary Medicine, Veterinary Institute for Regenerative Cures, University of California, Davis, Davis, California.

produce neocartilage with morphological, biochemical, and biomechanical properties akin to native hyaline cartilage.<sup>11</sup> Traditionally, primary juvenile chondrocytes are used as the cell source for self-assembly protocols; juvenile chondrocytes are more chondrogenic than adult chondrocytes<sup>12</sup> and do not require pretreatment to induce chondrogenesis, as is the case for progenitor populations such as mesenchymal stem cells (MSCs) or embryonic stem cells.<sup>13</sup> Unfortunately, the scarcity of juvenile cartilage donor tissue limits the translational potential of this approach, which has led us to turn to more readily available progenitor cells as an alternative cell source.

Although they require an additional step of chondrodifferentiation, MSCs offer a particularly attractive cell source for cartilage engineering. MSCs are isolated from various tissue sources, such as umbilical tissue, cord blood, Wharton's jelly, placenta, as well as several other adult somatic tissues, such as adipose and bone marrow. These MSCs can then be subsequently expanded to obtain sufficient cell numbers. MSCs also possess immunomodulatory properties and have been shown to be nonimmunogenic in both autologous and allogeneic applications.<sup>14–16</sup> Bone marrow-derived MSCs (BM-MSCs) have been most extensively characterized for musculoskeletal tissue engineering compared to other MSC sources;<sup>17–19</sup> however, recent literature suggests that cord blood MSCs (CB-MSCs) may elicit a more robust chondrogenic phenotype.<sup>20,21</sup>

Based on the relative availability and intrinsic chondrogenic properties of MSCs, we explored two sources of MSCs as potential candidates for MSC-based tissue engineering of articular cartilage using the self-assembling process. We hypothesized that both BM-MSCs and CB-MSCs would be amenable to self-assembly, however, CB-MSCs would generate neocartilage with properties more closely resembling that of native equine articular cartilage. With this study we hope to establish the superior MSC source to be carried forward in subsequent studies aimed at optimizing self-assembly protocols and ultimately generating neocartilage suitable for therapeutic purposes in equine joint repair. Moreover, as the equine is an ideal model for cartilage repair in humans, this work holds significant translational potential as well.<sup>22</sup>

## Materials and Methods

### *Cell isolation and expansion*

Equine BM-MSCs from three adult equine donors and CB-MSCs from three foals were collected at the University of California, Davis under an approved animal care and use protocol. BM-MSCs and CB-MSCs were processed and expanded to passage 1 (P1) as previously described<sup>23</sup> and stored in liquid nitrogen. Subsequently, BM-MSCs and CB-MSCs were further passaged to P6 in low-glucose Dulbecco's modified Eagle's medium (DMEM; Corning), 10% fetal bovine serum (FBS; Atlanta Biologicals), and 1% penicillin-streptomycin (Gibco). Passaging was performed using trypsinization with 0.05% trypsin EDTA (Gibco) upon reaching 90% confluency for each round of expansion.

Two of the three BM-MSC donors and two of the three CB-MSC donors were phenotyped through flow cytometry (Cytomics; Beckman Coulter FC500). Analysis of histo-

gram data (Supplementary Table S1; Supplementary Data are available online at [www.liebertpub.com/tea](http://www.liebertpub.com/tea)) and side scatter data (Supplementary Table S2) was performed using FlowJo flow cytometry software (Tree Star, Inc.). All MSC lines were confirmed to be positive (>71%) for MSC markers using antibodies directed against CD90 (clone DH24A; VMRD),<sup>24,25</sup> CD44 (clone CVS18; AbD Serotec),<sup>26</sup> and CD29 (clone 4B4LDC9LDH8; Beckman Coulter, Inc.).<sup>26</sup> All lines were confirmed to be negative for F6B (a pan leukocyte antibody, a generous gift from Dr. Jeffrey Stott, UCD, School of Veterinary Medicine)<sup>27</sup> and MHC II (clone CVS20; AbD Serotec).<sup>25</sup> MHC I was variably positive (clone CVS22; AbD Serotec).<sup>28</sup>

For isolation of equine articular chondrocytes (ACs), equine articular cartilage was obtained within 48 h post-mortem from five stillborn neonatal horses. Cartilage was minced and digested in 0.2% collagenase type II (Worthington) with 3% FBS (Atlanta Biologicals) in DMEM, high glucose, GlutaMAX™ (Gibco) for 18 h at 37°C. Cells were filtered with a 70 µm filter (Corning) and stored in liquid nitrogen in 10% dimethyl sulfoxide (DMSO) and 90% FBS until use. Chondrocytes were expanded to P3 in chemically defined chondrogenic culture medium<sup>29</sup> (CHG), consisting of DMEM, high glucose, GlutaMAX Supplement (Gibco), 1% penicillin-streptomycin-fungizone (BD Biosciences), 1% ITS+premix (BD Biosciences), 1% nonessential amino acids (Gibco), 100 nM dexamethasone, 50 µg/mL ascorbate-2-phosphate, 40 µg/mL L-proline, and 100 µg/mL sodium pyruvate. CHG was supplemented with 2% FBS, 1 ng/mL TGF-β1 (Peprotech), 10 ng/mL platelet-derived growth factor (PDGF; Peprotech), and 5 ng/mL basic fibroblastic growth factor (bFGF; Peprotech),<sup>30</sup> during expansion in monolayer culture.

### *Native tissue collection*

Equine patellas were harvested from three skeletally mature horses euthanized for reasons unrelated to musculoskeletal pathology. Intact stifle joints were collected within 48 h of death. Joints were opened, and six biopsy punches of articular cartilage were isolated from the patellar surface. Cartilage samples were washed in phosphate buffered saline (PBS) and wrapped in gauze soaked in PBS containing protease inhibitor containing 10 mM N-ethylmaleimide (Sigma) and 1 mM phenylmethylsulfonyl fluoride (Sigma) and frozen at -20°C until further analysis.

### *Postexpansion chondrogenic differentiation*

After expansion, BM-MSCs and CB-MSCs were differentiated, and ACs were redifferentiated to a chondrogenic phenotype using aggregate redifferentiation<sup>31</sup> for 7 days. During aggregate redifferentiation, cells were maintained in nonadherent, agarose-coated plates (2% agarose [Fisher Scientific] in PBS) at 750,000 cells/mL in CHG, supplemented with 10 ng/mL TGF-β1 (Peprotech), 100 ng/mL GDF-5 (Peprotech), and 100 ng/mL BMP-2A (Peprotech).<sup>31</sup> Plates were placed on an orbital shaker at 55 rpm for the first 24 h postseeding and then maintained in static culture at 37°C and 5% CO<sub>2</sub>, during which time cells coalesced to form aggregates. Medium was changed every other day. After 7 days, aggregates were digested for 45 min in 0.05% Trypsin-EDTA, followed by 30 min in 0.2% collagenase

type II solution, and filtering through a 70  $\mu\text{m}$  membrane (as described above). Digestion resulted in single-cell suspensions of BM-MSCs, CB-MSCs, and ACs. The three donors for each cell type were combined in equal parts to create the cell suspension used for neocartilage formation.

#### *Neocartilage self-assembly*

Neocartilage was formed using the self-assembling process in nonadherent agarose wells.<sup>11</sup> To create the wells, a sterilized mold consisting of 5 mm stainless steel posts was immersed in a 48-well plate containing 900  $\mu\text{L}$  per well of sterile molten 2% agarose in PBS. After the agarose solidified, the mold was removed and the agarose wells were washed thrice with CHG over a 48 h period. For neocartilage formation,  $2 \times 10^6$  cells were added to each well in 100  $\mu\text{L}$  of CHG supplemented with 200 U/mL hyaluronidase type I-S from bovine testes (Sigma) and 2  $\mu\text{M}$  cytochalasin D (Sigma). An additional 400  $\mu\text{L}$  of CHG with 2  $\mu\text{M}$  cytochalasin D was added to each well 4 h after seeding. Plates were maintained at 37°C and 10%  $\text{CO}_2$ . The medium was exchanged every 24 h for the first 7 days. For the first 72 h, CHG was supplemented with 2  $\mu\text{M}$  cytochalasin D. After 7 days, neocartilage constructs were unconfined from the agarose wells, transferred to a 24-well non-TCP plate, and fed with 1 mL of CHG every other day. At 28 days post initial seeding, constructs were tested biomechanically, and portions of each construct were collected for biochemical and histological analysis. Constructs were generated from ACs solely for use as a control for the alkaline phosphatase assay, as this assay requires tissue culture medium and the native equine cartilage tested in this study was not cultured.

#### *Mechanical construct evaluation*

Mechanical properties of constructs were assessed in tension and compression. Tensile testing was conducted using a TestResources 840L (TestResources). Samples were strained uniaxially at a constant strain rate of 1%/s. Young's modulus ( $E^Y$ ) and ultimate tensile strength (UTS) were evaluated using a custom MATLAB program (Mathworks). Compressive testing was performed under unconfined compression using an Instron 5565 (Instron). Biopsy punches of 2 mm diameter were taken from native tissue or constructs for compression testing. Samples were preconditioned with 15 cycles of 5% compressive strain and then tested under incremental stress relaxation at 10% and 20%. A Kelvin standard linear solid viscoelastic model was used to fit the data to establish the instantaneous modulus ( $E^I$ ) and relaxation modulus ( $E^r$ ) at each strain level.<sup>32</sup>

#### *Biochemical construct evaluation*

Tissues were evaluated biochemically for collagen content, glycosamino-glycan (GAG) content, and cellularity. Samples were weighed before and after lyophilization and digested in 125  $\mu\text{g}/\text{mL}$  papain (Sigma) in 50 mM phosphate buffer (pH 6.5) containing 2 mM N-acetyl cysteine (Sigma) and 2 mM ethylenediaminetetraacetic acid (Acros Organics) for 18 h at 60°C. Collagen content was quantified using a modified, perchloric acid-free, chloramine-T hydroxyproline assay with a Sircol™ type I collagen standard (Accurate Chemical).<sup>33</sup>

GAG content was measured using the Blyscan 1, 9-dimethylmethylene blue binding assay (Accurate Chemical). DNA was quantified using the Quant-iT™ PicoGreen® Assay (Invitrogen). The cell content of each construct was determined by assuming 7.7 pg DNA per cell. Alkaline phosphatase activity was measured in conditioned medium collected 48 h postfeeding. Conditioned medium samples were incubated for 1.5 h with 10 mM p-nitrophenyl phosphate (Sigma) in a solution of 1.5 M Tris (Sigma), 1 mM  $\text{MgCl}_2$  (Sigma), and 1 mM  $\text{ZnCl}_2$  (Sigma) at pH 9.6. The alkaline phosphatase activity was measured spectrophotometrically at 405 nm and was referred to a standard curve made from p-nitrophenol (Sigma). Medium from constructs generated from ACs was utilized as a reference rather than native equine cartilage for the alkaline phosphatase assay.

#### *Histological and immunohistochemical evaluation*

Samples of native equine patellar cartilage and samples of MSC neocartilage collected after 4 weeks in culture were fixed in 10% neutral-buffered formalin, paraffin-embedded, and sectioned at 6  $\mu\text{m}$ . Sections were stained with hematoxylin and eosin (H&E), Safranin-O/Fast-Green, and picrosirius red. For collagen immunohistochemistry, rabbit anti-type I collagen polyclonal antibody (ab34710) was used at 1:300 dilution (Abcam), and mouse monoclonal anti-type X collagen antibody (ab49945) was used at 1:200 dilution (Abcam) following antigen retrieval with citric acid (pH 6) at 95°C for 20 min and at room temperature for an additional 20 min. Rabbit anti-human type II collagen polyclonal antibody (ab34712) at a 1:600 dilution (Abcam) was used following antigen retrieval using 4 mg/mL hyaluronidase (Sigma) in PBS for 30 min followed by 3 mg/mL pepsin (Sigma) in 0.5% acetic acid for 30 min. Primary antibodies were incubated with the sections overnight at 4°C, followed by application of a species specific, conjugated secondary antibody (Vector Laboratories) and DAB staining (Vector Laboratories).

Following staining, images obtained from bone marrow and cord blood sections were processed using ImageJ to quantify the percentage of the tissue section that showed positive DAB staining. To perform this quantitative analysis, images were converted to an 8-bit image type and then inverted. Image threshold was adjusted to a B&W scale such that black areas corresponded to areas where DAB staining was present and white areas corresponded to nonstained areas. Construct edges were manually selected, and the fraction of the selected area that was black after image processing was measured and reported as a percentage of the selected area. For each collagen antibody 5 tissue sections were analyzed for each MSC group (Bone Marrow and Cord Blood). Areas where the tissue was folded were excluded from this analysis.

#### *Functionality index calculation*

The overall tissue quality was quantified by calculating a functionality index (*FI*) (Equation 1) that equally weighs GAG content, collagen content, compressive properties, and tensile properties of neocartilage relative to those of native tissue. The *FI* yields a score of 1.0 when neocartilage properties are equivalent to those of native tissue.

$$FI = \frac{1}{4} \left( 1 - \frac{(GAG_{NT} - GAG_{NC})}{GAG_{NT}} \right) + \frac{1}{4} \left( 1 - \frac{(Col_{NT} - Col_{NC})}{Col_{NT}} \right) + \frac{1}{4} \left( \left( 1 - \frac{(E'_{NT} - E'_{NC})}{E'_{NT}} \right) + \left( 1 - \frac{(E^i_{NT} - E^i_{NC})}{E^i_{NT}} \right) \right) + \frac{1}{4} \left( \left( 1 - \frac{(E^y_{NT} - E^y_{NC})}{E^y_{NT}} \right) + \left( 1 - \frac{(UTS_{NT} - UTS_{NC})}{UTS_{NT}} \right) \right)$$

In Equation (1), the *FI* quantifies the overall quality of tissue engineered neocartilage (subscript “*NC*”) compared to native equine articular cartilage (subscript “*NT*”) by equally weighing the GAG/dry weight (DW) (*GAG*), collagen content/DW (*Col*), compressive properties consisting of relaxation (*E'*) and instantaneous (*E<sup>i</sup>*) moduli, and tensile properties consisting of Young’s modulus (*E<sup>y</sup>*) and *UTS*.

*Statistical analysis*

All data are presented as mean ± standard deviation. Biochemical and mechanical properties were analyzed using one-way analysis of variance, followed by Tukey’s *post hoc* test where warranted. In figures 2 and 3 presenting mechanical and biochemical data, groups marked by different letters are statistically different (*p* < 0.05). Student’s *t*-test was performed to assess differences in thickness, diameter, cellularity, percent area stained and *FI* between BM-MSCs and CB-MSCs. In figures 1, 3, 5, and 6 corresponding to these properties, groups marked by a starred bar are statistically different (*p* < 0.05).

**Results**

*Gross morphology*

Both BM-MSCs and CB-MSCs were able to undergo expansion, chondrogenic differentiation through aggregate redifferentiation, and the self-assembling process to produce neocartilage constructs (Fig. 1A). BM-MSCs produced

constructs with significantly smaller diameter and thickness (*p* < 0.0001) than CB-MSC constructs. Although both cell types were initially seeded in 5 mm wells, the resultant BM-MSC constructs had an average diameter of 3.81 ± 0.07 mm, whereas CB-MSC constructs averaged 5.58 ± 0.07 mm in diameter (Fig. 1B). In terms of thickness, BM-MSC constructs averaged 0.21 ± 0.02 mm, while CB-MSC averaged 0.64 ± 0.03 mm (Fig. 1C). BM-MSC constructs were generally flat, whereas CB-MSC constructs had a shallow bowl-like conformation (Fig. 1A).

*Mechanical properties*

Cylindrical punches from each sample were tested in a displacement-controlled, unconfined compression mode, yielding relaxation and instantaneous moduli. For comparison, native tissue from the equine patella was tested in parallel. The instantaneous modulus upon 20% strain was 339 ± 129 kPa, 1178 ± 192 kPa, and 1377 ± 375 kPa for BM-MSC constructs, CB-MSC constructs, and native tissue, respectively (Fig. 2A). The relaxation modulus values were 81 ± 21 kPa, 291 ± 59 kPa, and 396 ± 157 kPa for BM-MSC constructs, CB-MSC constructs, and native tissue, respectively (Fig. 2B).

Tensile properties were measured by performing a uniaxial strain-to-failure test. Again, equine patellar tissue was used to obtain native tissue values. The Young’s modulus values were 4.9 ± 1.1 MPa, 2.8 ± 1.1 MPa, and 9.6 ± 3.8 MPa for BM-MSC constructs, CB-MSC constructs, and native tissue, respectively

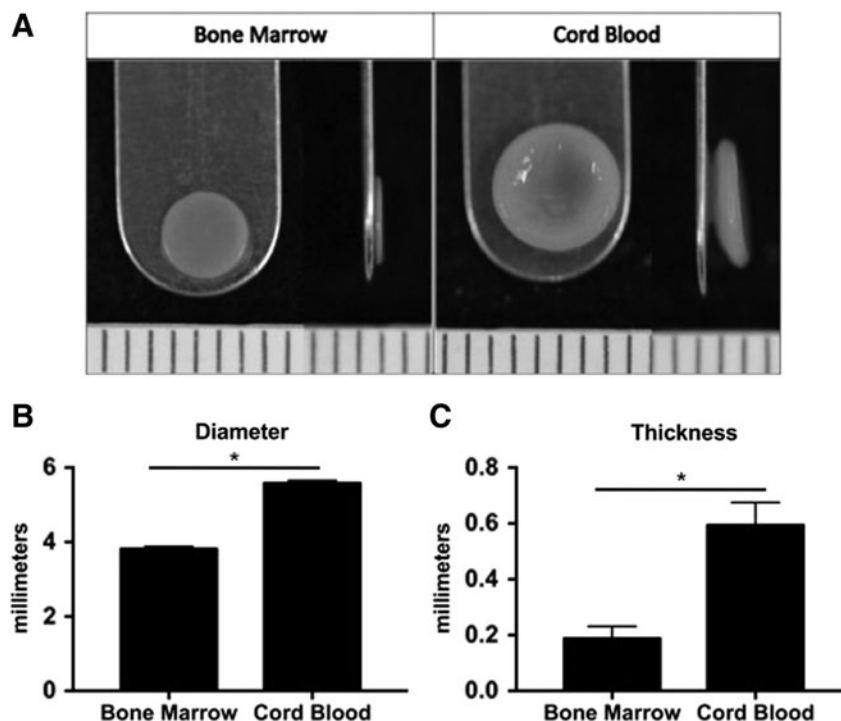


**FIG. 1.** Construct gross morphology and dimensions presented as mean ± standard deviation in millimeters. Student’s *t*-test was performed using *p* < 0.05 as statistical significance; *starred bars* show statistical significance between groups. (A) Representative images of BM-MSC constructs (Bone Marrow) and CB-MSC constructs (Cord Blood). BM-MSCs generated constructs that were generally flatter than CB-MSCs. CB-MSC constructs were significantly wider (B) and thicker (C) compared to BM-MSC constructs. BM-MSC, bone marrow-derived mesenchymal stem cells; CB-MSC, cord blood mesenchymal stem cell.

**FIG. 2.** Mechanical properties of BM-MSC and CB-MSC constructs, as well as native equine articular cartilage (Native Tissue). One-way ANOVAs were performed using  $p < 0.05$  for statistical significance; letters above the bars show statistical significance between groups. In terms of compressive properties, both the instantaneous modulus (A) and relaxation modulus (B) were higher in CB-MSC constructs compared to BM-MSC constructs. Native tissue and Cord Blood did not significantly differ for either compressive property as well. BM-MSCs yielded constructs that had both higher tensile stiffness, represented by Young's modulus (C), and ultimate tensile strength (D) compared to CB-MSCs. ANOVAs, analyses of variance.

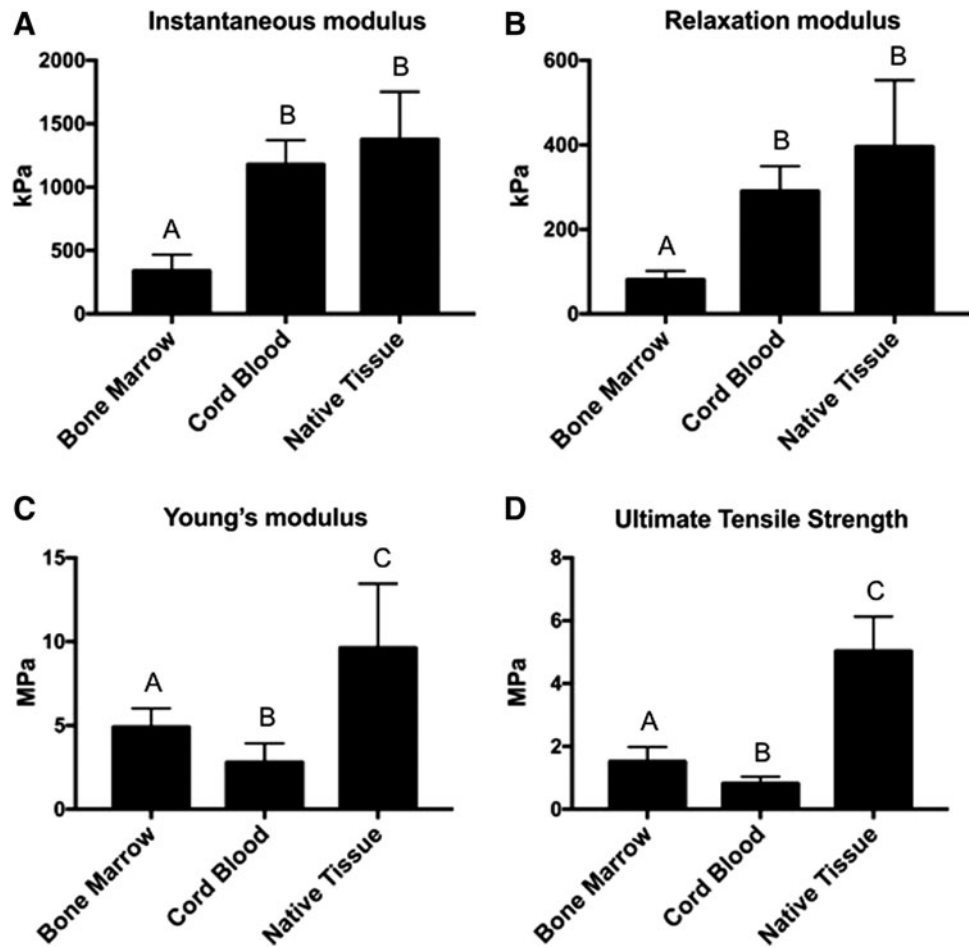


(Fig. 2C). The *UTS* was determined to be  $1.5 \pm 0.5$  MPa for BM-MSC constructs,  $0.8 \pm 0.2$  MPa for CB-MSC constructs, and  $5.0 \pm 1.1$  MPa for native tissue (Fig. 2D).

#### Biochemical properties

Water, collagen, GAG, and DNA content were measured for each sample. The water content values were  $77.0\% \pm 1.9\%$ ,  $83.9\% \pm 0.8\%$ , and  $77.3\% \pm 0.5\%$  for BM-MSC constructs, CB-MSC, and native tissue, respectively (Fig. 3A). Collagen per DW was  $0.27 \pm 0.02$  mg/mg,  $0.13 \pm 0.02$  mg/mg, and  $0.53 \pm 0.06$  mg/mg (Fig. 3B), while GAG/DW was  $0.038 \pm 0.003$  mg/mg,  $0.150 \pm 0.010$  mg/mg, and  $0.168 \pm 0.009$  mg/mg for BM-MSC constructs, CB-MSC constructs, and native tissue, respectively (Fig. 3C). Alkaline phosphatase activity was measured in the supernatant from constructs produced using BM-MSCs, CB-MSCs, as well as equine ACs for comparison. Alkaline phosphatase activity, expressed as units of alkaline phosphatase normalized to total protein content, was  $0.042 \pm 0.007$  U/mg,  $0.010 \pm 0.001$  U/mg, and  $0.009 \pm 0.001$  U/mg for BM-MSC constructs, CB-MSC constructs, and AC constructs, respectively (Fig. 3D). Although both BM-MSCs and CB-MSCs were seeded at a density of 2 million cells per self-assembly well, the resulting BM-MSC constructs contained  $0.63 \pm 0.11$  million cells after 28 days, while CB-MSC constructs contained  $1.14 \pm 0.06$  million cells at day 28 (Fig. 3E).

#### Histology and immunohistochemistry

Formalin fixed, paraffin embedded sections were processed and sectioned for both histological and immunohistochemical staining. H&E was used to assess general tissue composition, structure, and cellularity. Picrosirius red and Safranin-O/Fast-Green were used to qualitatively evaluate collagen and GAG distribution, respectively. Overall, the results of the histology suggest that CB-MSCs produced tissue that more closely resembled native equine articular cartilage, with a GAG-rich matrix surrounding cells within lacunae (Fig. 4). BM-MSC constructs, on the other hand, produced very little GAG and fewer lacuna-like structures. BM-MSC constructs showed higher stain uptake for Sirius red compared to CB-MSC constructs, suggesting greater overall collagen content (Fig. 4).

Immunohistochemistry was performed to determine the type of collagen being synthesized and whether these constructs displayed the collagen type II-rich composition that is characteristic of hyaline articular cartilage. Quantification of DAB staining on representative tissue section images revealed that BM-MSC constructs had positive collagen type I on  $26.3\% \pm 5.0\%$  of the total construct area, whereas CB-MSC constructs had significantly less with  $6.8\% \pm 1.6\%$ . Conversely, BM-MSC constructs had a significantly smaller area of collagen type II compared to CB-MSC constructs,  $21.0\% \pm 6.6\%$  and  $51.2\% \pm 12.9\%$ , respectively. Collagen type X immunohistochemistry was used to assess whether

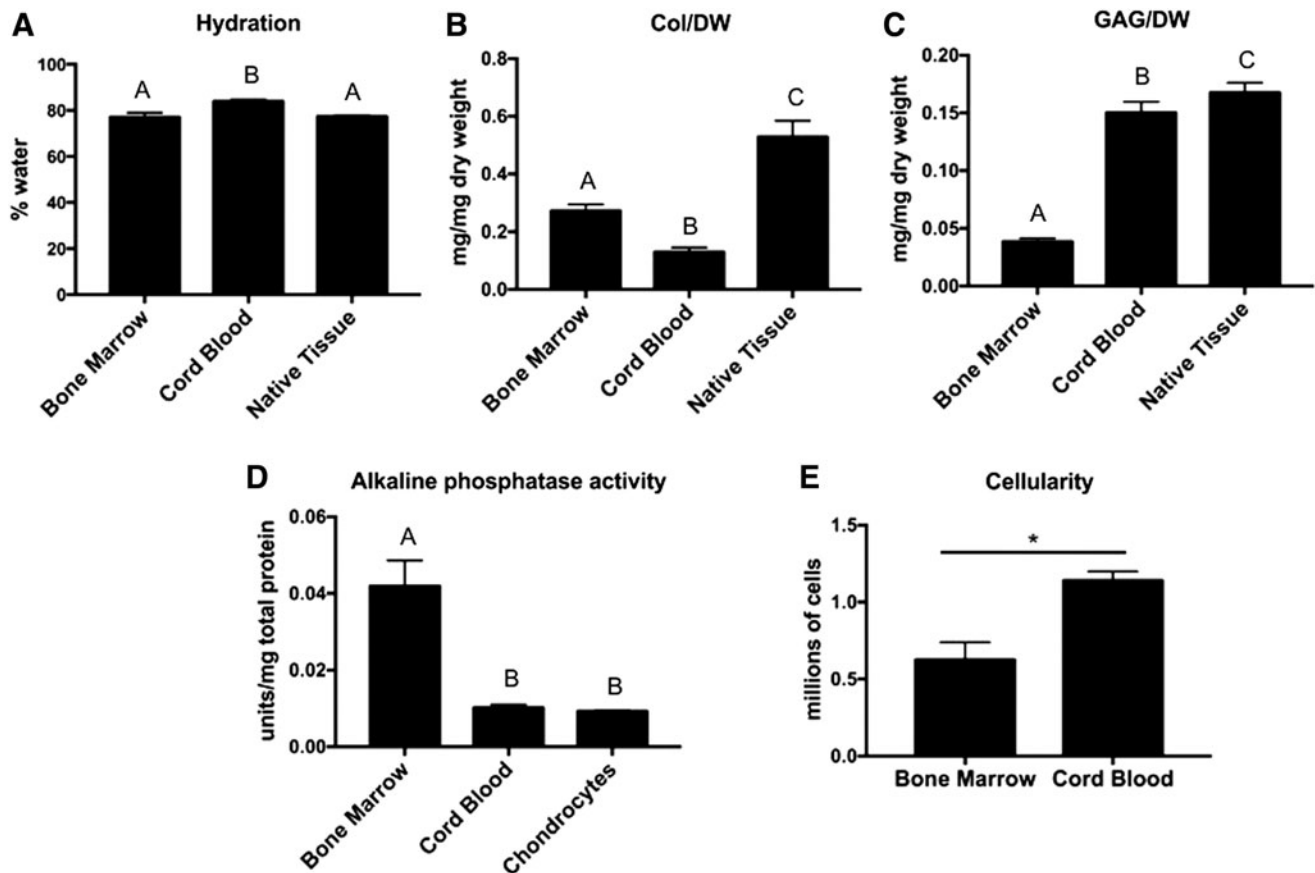


**FIG. 3.** Biochemical properties of both construct groups (Bone Marrow and Cord Blood) and Native Tissue or equine AC-derived tissue (Chondrocytes) in the case of alkaline phosphatase activity. One-way ANOVAs were performed for all assays except Cellularity using  $p < 0.05$  for statistical significance; letters above the bars show statistical significance between groups. Hydration did not differ significantly between Native Tissue and Bone Marrow, while Cord Blood had significantly higher hydration than both groups (A). Collagen/WW basis was significantly higher in Bone Marrow compared to Cord Blood, but both construct groups were significantly lower than Native Tissue (B). GAG/WW was significantly higher in Cord Blood compared to Bone Marrow; however, both of these groups were lower than Native Tissue (C). Cord Blood constructs produced alkaline phosphatase at levels comparable to that of constructs derived from passaged equine ACs. Bone Marrow constructs produced significantly higher levels suggesting a further progression in hypertrophy (D). Cellularity was compared using a Student's  $t$ -test with  $p < 0.05$  as statistical significance; the starred bar shows statistical significance between groups. Cord Blood constructs contained more cells than Bone Marrow constructs despite an equal initial seeding density of 2 million cells per construct (E). AC, articular chondrocyte; WW, wet weight.

the cells had progressed to a hypertrophic phenotype as a result of the self-assembling process. BM-MSC constructs had a significantly greater area of positive collagen type X staining with  $79.9\% \pm 12.2\%$  compared to CB-MSC constructs, which had a positive area of  $12.4\% \pm 4.1\%$  (Fig. 5).

#### Functionality index

BM-MSC constructs yielded an  $FI$  of  $0.34 \pm 0.04$ , which was significantly lower than CB-MSC constructs, which yielded an  $FI$  of  $0.54 \pm 0.05$  ( $p < 0.0001$ ; Fig. 6). By this measure, CB-MSC constructs were deemed superior to BM-MSC constructs for generating neocartilage through the self-assembling process.

#### Discussion

The cartilage-like ECM produced by chondrodifferentiated MSCs holds potential as a cartilage tissue replacement if it can be shown to replicate salient native tissue

properties, especially those related to the tissue's ability to withstand the strenuous loading environment of a diarthrodial joint. Using  $FI$ , a quantitative index representing these salient properties, this study compared biochemical and biomechanical properties of scaffold-free tissues engineered from BM-MSCs and CB-MSCs against the properties of native articular cartilage. Equine BM-MSCs or CB-MSCs were expanded, chondrodifferentiated, self-assembled into neocartilage constructs, cultured for 4 weeks, and assayed. Based on previous studies,<sup>20,21</sup> it was hypothesized that, compared to BM-MSCs, CB-MSCs would produce more hyaline-like tissue (i.e., CB-MSCs would generate constructs with a higher  $FI$ ). This hypothesis was supported by the data.

CB-MSC constructs possessed higher compressive properties and GAG content than BM-MSC constructs. Although BM-MSC constructs possessed higher tensile properties and collagen content, its  $FI$  was nonetheless lower than CB-MSC constructs. BM-MSC constructs produced more alkaline phosphatase and collagen type X, suggesting a hypertrophic

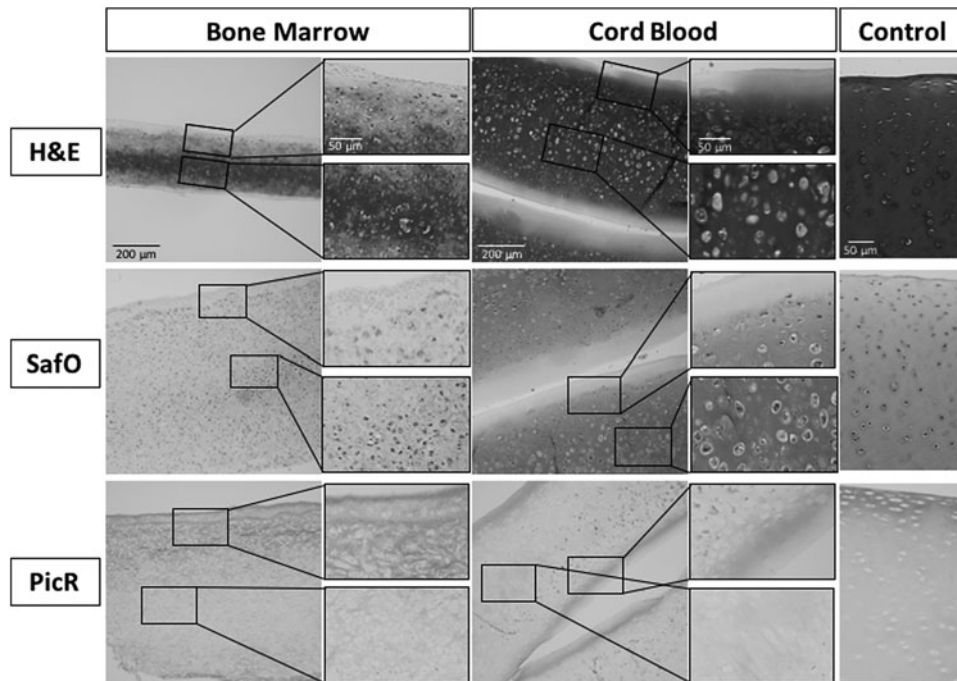


**FIG. 4.** Representative histology images of Bone Marrow constructs, Cord Blood constructs, and equine patellar cartilage (Control). For each section a low magnification image is presented on the *left* with higher magnification images corresponding to the *black boxed* regions on the *right*. Scale bars are presented in the *top image* of each *column*: 200  $\mu\text{m}$  for low magnification images, 50  $\mu\text{m}$  for high magnification and Control images. H&E staining highlights the lacuna structures and hematopylin intense staining representative of articular cartilage in both the native tissue Control and Cord Blood groups; however, these characteristics are largely absent in the Bone Marrow group. Picosirius red (PicR) highlights the collagen content, which had higher stain uptake in Bone Marrow compared to Cord Blood, whereas Safranin-O (SafO) with a Fast-Green counterstain highlights GAG content, which had higher stain uptake in Cord Blood. H&E, hematoxylin and eosin.

phenotype that is not suitable for articular cartilage implants. CB-MSC constructs produced quantities of alkaline phosphatase that were similar to those of constructs from passaged ACs and higher quantities of collagen type II compared to collagen type I. Taken together, the data showed that CB-MSC constructs more closely resembled native equine articular cartilage, with an *FI* significantly closer to 1.0, compared to BM constructs. This study showed that CB-MSCs were superior to BM-MSCs for the purpose of generating scaffold-free cartilage using the self-assembling process. Importantly, this study provided the first source of comprehensive mechanical properties for scaffold-free cartilage generated from MSC sources.

Mechanical characterization of scaffold-free neocartilage generated from MSCs revealed that the mechanical properties of neotissues are a function of the source of MSCs used. BM-MSCs produced constructs that were 1.85 $\times$  stronger and 1.75 $\times$  stiffer in tension compared to CB-MSC constructs, whereas CB-MSCs produced constructs with significantly higher compressive stiffness compared to BM-MSC constructs. The relaxation modulus and instantaneous modulus of CB-MSC constructs were 3.59 $\times$  and 3.47 $\times$  higher than those of BM-MSC constructs, respectively. The mechanical properties of MSC-derived constructs were comparable to those of scaffold-free constructs formed using chondrocytes, costal chondrocytes, and fibrochondrocytes.<sup>10,34,35</sup> Although mechanical properties have been measured for MSC constructs seeded in various scaffold,

to the authors' knowledge, this is the first study to measure both compressive and tensile properties of MSC-derived, scaffold-free neocartilage.

The self-assembled neocartilage generated from MSCs in this study possessed mechanical properties comparable to those of native equine articular cartilage. Compressive properties of CB-MSC constructs were remarkably close to those of native tissue; both the relaxation modulus and instantaneous moduli of CB-MSC constructs did not differ significantly from those of equine patellar cartilage. This finding has direct clinical implications as treatments for patellar cartilage lesions are fewer and associated with inferior clinical outcomes compared to other compartments of the knee. As a result, novel treatments for the patellar indication are needed, and a trend toward the use of cell-based therapies has been observed.<sup>37</sup> Moreover, topographic characterizations of equine (unpublished data) and ovine<sup>38</sup> distal femur cartilage, including the patella, condyles, and trochlea, have shown that the biomechanical and biochemical properties of patellar cartilage are comparable to cartilage from weight bearing regions of the joint. This finding, taken in conjunction with the results of this study, suggests that CB-MSCs are a suitable cell source for generating self-assembled constructs with properties that can withstand the natural compressive loading environment following a 4-week *in vitro* maturation process.

In conjunction with the significant differences found in mechanical properties between BM-MSC and CB-MSC

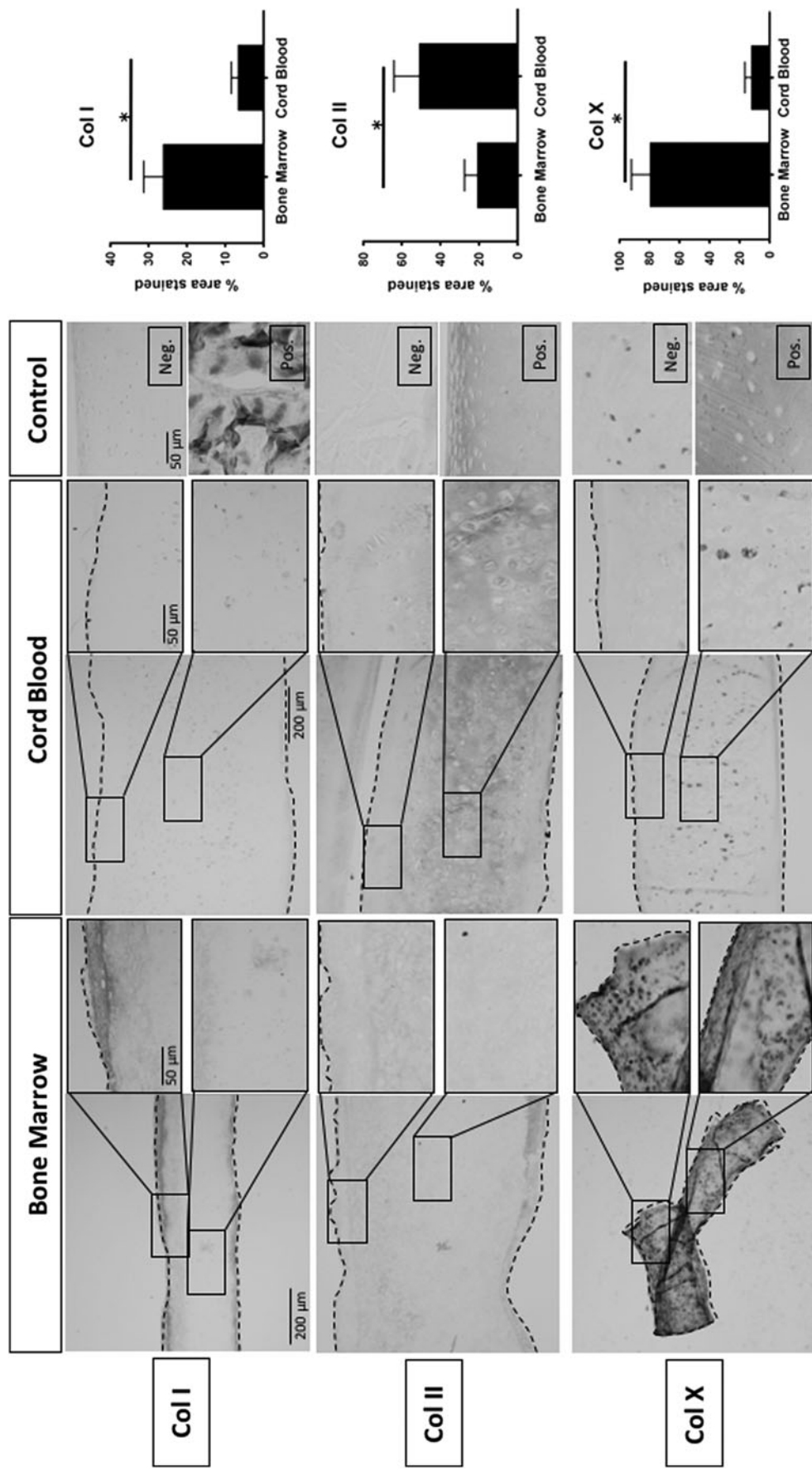


**FIG. 5.** Representative immunohistochemistry images and stain quantification of Bone Marrow constructs, Cord Blood constructs, and positive and negative native tissue controls. For each tissue section, a low magnification image is presented on the *left* with higher magnification images corresponding to the *black boxed* regions on the *right*. *Dashed lines* define construct edges. Scale bars are presented in the *top image* of each *column* and reflect the scale for all images in the *column*: 200 μm for low magnification images, 50 μm for high magnification and Control images. The percentage of the tissue section that showed DAB staining was quantified and presented as percent area stained for each antibody (*right*). Student's *t*-test was performed using  $p < 0.05$  as statistical significance; *starred bars* show statistical significance between groups. Equine tendon was used as a positive control and equine articular cartilage as a negative control for collagen type I staining (Col I). Bone Marrow constructs had higher levels of staining for this marker of fibrocartilage. Equine articular cartilage was a positive control, and equine tendon was a negative control for collagen type II staining (Col II). Cord Blood constructs possessed higher levels of stain for this hyaline cartilage marker. Osteoarthritic equine articular cartilage served as a positive control, while nonarthritic equine articular cartilage served as a negative control for collagen type X (Col X). Bone Marrow constructs had higher stain uptake for this marker of hypertrophic cartilage.



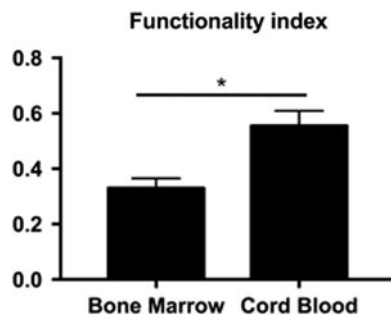


**FIG. 6.** A quantitative functionality index comprised Collagen/WW, GAG/WW, compressive, and tensile properties; a value of 1.0 is equivalent to equine patellar articular cartilage properties. Student's *t*-test was performed using  $p < 0.05$  as statistical significance; *starred bars* show statistical significance between groups. Cord Blood had a score closer to 1.0 and was significantly higher than Bone Marrow.

constructs, biochemical and histological properties also differed significantly between these two groups. CB-MSCs produced GAG at levels comparable to that of native tissue and 2.86× higher compared with BM-MSC, and explains, in part, why CB-MSC construct compressive properties were much closer to those of native tissue compared to those of BM-MSC constructs. The GAG content of cartilage is responsible for imparting the tissue with its resilience to compressive forces by attracting and retaining water within the matrix.<sup>39</sup> BM-MSC constructs, in contrast, had 2.08× higher total collagen content compared to CB-MSC constructs, although this amount was still only 51% of native tissue content.

The amount, organization, and degree of cross-linking of collagen all play crucial roles in the tensile integrity of cartilage.<sup>39</sup> Therefore, in light of differences in collagen content, it is not surprising that BM-MSC constructs possessed higher tensile properties compared to CB-MSC constructs. When examining the specific types of collagen present in the constructs, however, we found that CB-MSC constructs contained more collagen type II and less collagen type I than BM-MSC constructs, indicating that CB-MSCs produced a more hyaline-like tissue. This is supported by the findings of greater amounts of collagen type X and significantly higher alkaline phosphatase activity seen in BM-MSC constructs, indicative of the BM-MSCs' progression to a hypertrophic phenotype. Overall, the biochemical and histological properties are consistent with the mechanical data, and all data suggest that, compared to BM-MSCs, CB-MSCs produce a tissue more similar to native equine articular cartilage.

In developing protocols for cartilage repair using novel cell sources, issues of immunomodulation and phenotypic stability are of paramount importance. MSCs can be harvested from autologous or allogeneic sources, mitigating the issue of donor site morbidity associated with tissue harvest. Use of an allogeneic cell source carries the risk of generating a host immune response; however, MSCs have been shown to exhibit immunomodulatory properties.<sup>40,41</sup> While it is not fully understood to what extent these properties are maintained upon differentiation, recent studies suggest that these properties may not be lost upon chondrodifferentiation. For example, a study of the immunomodulatory properties of CB-MSCs demonstrated that chondrodifferentiation of these cells

did not increase antigenicity, and immunomodulatory properties were maintained upon differentiation to a chondrocyte phenotype.<sup>42</sup> Likewise, MSCs from adipose tissue and bone marrow were also shown to maintain their immunosuppressive properties upon chondrogenic differentiation.<sup>43</sup> Thus, in regard to immunosuppression and immunomodulation, both BM-MSCs and CB-MSCs show promise as potential cell sources for cartilage repair.

In addition to the issue of immune system interaction, the question also remains as to the ability to which MSCs can maintain a stable chondrogenic phenotype upon *in vivo* implantation. Several treatments that aimed at preventing terminal differentiation of chondrogenic BM-MSCs have been attempted, to various degrees of success<sup>44-46</sup>; however, it is yet to be determined whether MSCs that have been chondrodifferentiated before implantation can result in long-term cartilage repair.<sup>18</sup> The majority of cartilage repair attempts using MSCs have utilized BM-MSCs; however, based on the results of the alkaline phosphatase and collagen X assays of this study, BM-MSCs may not be the ideal MSC source. While CB-MSCs may generate neotissues that are more similar to hyaline articular cartilage than BM-MSCs, further studies will be necessary to establish long-term phenotypic stability and immunomodulatory properties in an appropriate animal model.

In this study, MSCs were chondrodifferentiated using an aggregate redifferentiation method and tissue engineered using the self-assembling process. Aggregate redifferentiation recapitulates the developmental process of MSC condensation and chondrodifferentiation by culturing the cells in a suspension culture system and applying growth factors to promote chondrogenesis.<sup>31</sup> The self-assembling process is a scaffold-free technique for generating cartilage repair grafts,<sup>11</sup> and by avoiding the use of scaffolds, issues such as stress shielding, interference with integration of surrounding native tissue, scaffold biocompatibility, and degradation by-products are precluded.<sup>10</sup> The self-assembling process has generated robust neocartilage with properties comparable to those of native cartilage using chondrocytes, BM-MSCs and CB-MSCs, as well as other progenitor cell populations.<sup>47</sup>

Although only BM-MSCs and CB-MSCs were utilized in this study, it is likely that MSCs from other sources could be used. The quality of self-assembled neocartilage, however, will, in part, depend on the starting cell source and the degree to which the cells are chondrodifferentiated.<sup>31</sup> With this study, we showed that CB-MSCs resulted in overall superior constructs compared to BM-MSCs despite the fact that tensile properties and total collagen content of CB-MSC constructs were lacking compared to BM-MSC constructs. Therefore, future studies using CB-MSCs for cartilage self-assembly should aim to increase collagen content and collagen cross-linking to improve tensile properties. Bioactive factors such as TGF- $\beta$ 1, chondroitinase-ABC, and lysyl oxidase like protein-2 can be applied during the self-assembling process and have been shown to significantly increase collagen and hydroxyproline cross-linking content of neocartilage generated from fibrocartilage and articular cartilage-derived chondrocytes, and, therefore, may facilitate collagen production and cross-linking in MSCs as well.<sup>48,49</sup> As demonstrated in this study, MSCs can be robustly chondrodifferentiated using aggregate redifferentiation and are amenable to the self-assembling process; however,

efforts need to be exerted to improve upon the functional properties, especially under tension, to achieve full native tissue values.

In conclusion, this study represents the first use of CB-MSCs in a self-assembling process for cartilage tissue engineering. It is also the first study to fully characterize both compressive and tensile mechanical properties of scaffold-free tissue engineered cartilage from an MSC source. CB-MSCs proved to be superior overall, with an *FI* >50% of native equine patellar cartilage, as well as collagen production and alkaline phosphatase activity comparable to those of native equine articular cartilage.

### Acknowledgments

This project was supported by the Center for Equine Health with funds provided by the State of California satellite wagering fund and contributions by private donors, and the National Center for Advancing Translational Sciences, National Institutes of Health, through grant No. UL1 TR001860 and linked award TL1 TR001861. The content is solely the responsibility of the authors and does not necessarily represent the official views of the NIH.

### Disclosure Statement

No competing financial interests exist.

### References

- Yang, J., Tibbetts, A.S., Covassin, T., Cheng, G., Nayar, S., and Heiden, E. Epidemiology of overuse and acute injuries among competitive collegiate athletes. *J Athl Train* **47**, 198, 2012.
- Hootman, J.M., Dick, R., and Agel, J. Epidemiology of collegiate injuries for 15 sports: summary and recommendations for injury prevention initiatives. *J Athl Train* **42**, 311, 2007.
- Ristolainen, L., Heinonen, A., Turunen, H., *et al.* Type of sport is related to injury profile: a study on cross country skiers, swimmers, long-distance runners and soccer players. A retrospective 12-month study. *Scand J Med Sci Sports* **20**, 384, 2009.
- Penell, J.C., Egenvall, A., Bonnett, B.N., Olson, P., and Pringle, J. Specific causes of morbidity among Swedish horses insured for veterinary care between 1997 and 2000. *Vet Rec* **157**, 470, 2005.
- Desjardins, M.R., and Hurtig, M.B. Cartilage healing: a review with emphasis on the equine model. *Can Vet J* **31**, 565, 1990.
- Huey, D.J., Hu, J.C., and Athanasiou, K.A. Unlike bone, cartilage regeneration remains elusive. *Science* **338**, 917, 2012.
- Hurtig, M.B., Fretz, P.B., Doige, C.E., and Schnurr, D.L. Effect of lesion size and location on equine articular cartilage repair. *Can Vet J* **52**, 137, 1988.
- Convery, F.R., Akeson, W.H., and Keown, G.H. The repair of large osteochondral defects. An experimental study in horses. *Clin Orthop Relat Res* **82**, 253, 1972.
- de Windt, T.S., Bekkers, J.E.J., Creemers, L.B., Dhert, W.J.A., and Saris, D.B.F. Patient profiling in cartilage regeneration: prognostic factors determining success of treatment for cartilage defects. *Am J Sports Med* **37**, 58S, 2009.
- Athanasiou, K.A., Eswaramoorthy, R., Hadidi, P., and Hu, J.C. Self-organization and the self-assembling process in tissue engineering. *Annu Rev Biomed Eng* **15**, 115, 2013.
- Hu, J.C., and Athanasiou, K.A. A self-assembling process in articular cartilage tissue engineering. *Tissue Eng* **12**, 969, 2006.
- Smeriglio, P., Lai, J.H., Dhulipala, L., *et al.* Comparative potential of juvenile and adult human articular chondrocytes for cartilage tissue formation in three-dimensional biomimetic hydrogels. *Tissue Eng Part A* **21**, 147, 2015.
- Wang, M., Yuan, Z., Ma, N., *et al.* Advances and prospects in stem cells for cartilage regeneration. *Stem Cells Int* **11**, 4130607, 2017.
- Carrade Holt, D.D., Wood, J.A., Granick, J.L., Walker, N.J., Clark, K.C., and Borjesson, D.L. Equine mesenchymal stem cells inhibit T cell proliferation through different mechanisms depending on tissue source. *Stem Cells Dev* **23**, 1258, 2014.
- Carrade, D.D., and Borjesson, D.L. Immunomodulation by mesenchymal stem cells in veterinary species. *Comp Med* **63**, 207, 2013.
- Whitworth, D.J., and Banks, T.A. Stem cell therapies for treating osteoarthritis: prescient or premature? *Vet J* **202**, 416, 2014.
- Wang, L., Ott, L., Seshareddy, K., Weiss, M.L., and Detamore, M.S. Musculoskeletal tissue engineering with human umbilical cord mesenchymal stromal cells. *Regen Med* **6**, 95, 2011.
- Reissis, D., Tang, Q.O., Cooper, N.C., *et al.* Current clinical evidence for the use of mesenchymal stem cells in articular cartilage repair. *Expert Opin Biol Ther* **16**, 535, 2016.
- Liu, S., Yuan, M., Hou, K., *et al.* Immune characterization of mesenchymal stem cells in human umbilical cord Wharton's jelly and derived cartilage cells. *Cell Immunol* **278**, 35, 2012.
- Berg, L., Koch, T., Heerkens, T., Bessonov, K., Thomsen, P., and Betts, D. Chondrogenic potential of mesenchymal stromal cells derived from equine bone marrow and umbilical cord blood. *Vet Comp Orthop Traumatol* **22**, 363, 2009.
- Zhang, X., Hirai, M., Cantero, S., *et al.* Isolation and characterization of mesenchymal stem cells from human umbilical cord blood: reevaluation of critical factors for successful isolation and high ability to proliferate and differentiate to chondrocytes as compared to mesenchymal stem cells from bone marrow and adipose tissue. *J Cell Biochem* **112**, 1206, 2011.
- McIlwraith, C.W., Fortier, L.A., Frisbie, D.D., and Nixon, A.J. Equine models of articular cartilage repair. *Cartilage* **2**, 317, 2011.
- Toupadakis, C.A., Wong, A., Genetos, D.C., *et al.* Comparison of the osteogenic potential of equine mesenchymal stem cells from bone marrow, adipose tissue, umbilical cord blood, and umbilical cord tissue. *Am J Vet Res* **71**, 1237, 2010.
- Carrade, D.D., Lame, M.W., Kent, M.S., Clark, K.C., Walker, N.J., and Borjesson, D.L. Comparative analysis of the immunomodulatory properties of equine adult-derived mesenchymal stem cells. *Cell Med* **4**, 1, 2012.
- Carrade, D.D., Owens, S.D., Galuppo, L.D., *et al.* Clinicopathologic findings following intra-articular injection of autologous and allogeneic placental derived equine mesenchymal stem cells in horses. *Cytotherapy* **13**, 419, 2011.
- Radcliffe, C.H., Flaminio M.J.B.F., and Fortier, L.A. Temporal analysis of equine bone marrow aspirate during establishment of putative mesenchymal progenitor cell populations. *Stem Cells Dev* **19**, 269, 2010.

27. Watson, J.L., Stott, J.L., Blanchard, M.T., *et al.* Phenotypic characterization of lymphocyte subpopulations in horses affected with chronic obstructive pulmonary disease and in normal controls. *Vet Pathol* **34**, 108, 2016.
28. Carrade, D.D., Affolter, V.K., Outerbridge, C.A., *et al.* Intradermal injections of equine allogeneic umbilical cord-derived mesenchymal stem cells are well tolerated and do not elicit immediate or delayed hypersensitivity reactions. *Cytotherapy* **13**, 1180, 2011.
29. Johnstone, B., Hering, T.M., Caplan, A.I., Goldberg, V.M., and Yoo, J.U. In vitro chondrogenesis of bone marrow-derived mesenchymal progenitor cells. *Exp Cell Res* **238**, 265, 1998.
30. Murphy, M.K., Huey, D.J., Reimer, A.J., Hu, J.C., and Athanasiou, K.A. Enhancing post-expansion chondrogenic potential of costochondral cells in self-assembled neocartilage. *PLoS One* **8**, e56983, 2013.
31. Murphy, M.K., Huey, D.J., Hu, J.C., and Athanasiou, K.A. TGF- $\beta$ 1, GDF-5, and BMP-2 stimulation induces chondrogenesis in expanded human articular chondrocytes and marrow-derived stromal cells. *Stem Cells* **33**, 762, 2015.
32. Allen, K.D., and Athanasiou, K.A. Viscoelastic characterization of the porcine temporomandibular joint disc under unconfined compression. *J Biomech* **39**, 312, 2006.
33. Cissell, D.D., Link, J.M., Hu, J.C., and Athanasiou, K.A. A modified hydroxyproline assay based on hydrochloric acid in Ehrlich's solution accurately measures tissue collagen content. *Tissue Eng Part C Methods* **23**, 243, 2017.
34. Murphy, M.K., DuRaine, G.D., Reddi, A.H., Hu, J.C., and Athanasiou, K.A. Inducing articular cartilage phenotype in costochondral cells. *Arthritis Res Ther* **15**, R214, 2013.
35. MacBarb, R.F., Paschos, N.K., Abeug, R., Makris, E.A., Hu, J.C., and Athanasiou, K.A. Passive strain-induced matrix synthesis and organization in shape-specific, cartilaginous neotissues. *Tissue Eng Part A* **20**, 3290, 2014.
36. Huang, A.H., Farrell, M.J., and Mauck, R.L. Mechanics and mechanobiology of mesenchymal stem-cell based engineered cartilage. *J Biomech* **43**, 128, 2010.
37. Niemeyer, P., Feucht, M.J., Fritz, J., Albrecht, D., Spahn, G., and Angele, P. Cartilage repair surgery for full-thickness defects of the knee in Germany: indications and epidemiological data from the German Cartilage Registry (KnorpelRegister DGOU). *Arch Orthop Trauma Surg* **136**, 891, 2016.
38. Huwe, L.W., Brown, W.E., Hu, J.C., and Athanasiou, K.A. Characterization of costal cartilage and its suitability as a cell source for articular cartilage tissue engineering. *J Tissue Eng Regen Med*. [Epub ahead of print], 2017.
39. Athanasiou, K.A., Darling, E.M., Hu, J.C., DuRaine, G.D., and Reddi, A.H. *Articular Cartilage*. Boca Raton: CRC Press, 2017.
40. Regulski, M.J. Mesenchymal stem cells: guardians of inflammation. *Wounds* **29**, 20, 2017.
41. Uccelli, A., Moretta, L., and Pistoia, V. Immunoregulatory function of mesenchymal stem cells. *Eur J Immunol* **36**, 2566, 2006.
42. Lee, H.J., Kang, K.S., Kang, S.Y., *et al.* Immunologic properties of differentiated and undifferentiated mesenchymal stem cells derived from umbilical cord blood. *J Vet Sci* **17**, 289, 2016.
43. Du, W.J., Reppel, L., Leger, L., *et al.* Mesenchymal stem cells derived from human bone marrow and adipose tissue maintain their immunosuppressive properties after chondrogenic differentiation: role of HLA-G. *Stem Cells Dev* **25**, 1454, 2016.
44. Dickhut, A., Pelttari, K., Janicki, P., *et al.* Calcification or dedifferentiation: requirement to lock mesenchymal stem cells in a desired differentiation stage. *J Cell Physiol* **219**, 219, 2009.
45. Jeong, S.Y., Ha, J., Lee, M., *et al.* Autocrine action of thrombospondin-2 determines the chondrogenic differentiation potential and suppresses hypertrophic maturation of human umbilical cord blood-derived mesenchymal stem cells. *Stem Cells* **33**, 329, 2015.
46. Bian, L., Zhai, D.Y., Zhang, E.C., Mauck, R.L., and Burdick, J.A. Dynamic compressive loading enhances cartilage matrix synthesis and distribution and suppresses hypertrophy in hMSC-laden hyaluronic acid hydrogels. *Tissue Eng Part A* **18**, 715, 2012.
47. Lee, J.K., Link, J.M., Hu, J.C., and Athanasiou, K.A. The self-assembling process and applications in tissue engineering. *Cold Spring Harb Perspect Med* **7**, a025668, 2017.
48. Makris, E.A., MacBarb, R.F., Paschos, N.K., Hu, J.C., and Athanasiou, K.A. Combined use of chondroitinase-ABC, TGF-beta1, and collagen crosslinking agent lysyl oxidase to engineer functional neotissues for fibrocartilage repair. *Biomaterials* **35**, 6787, 2014.
49. Lee, J.K., Huwe, L.W., Paschos, N., *et al.* Tension stimulation drives tissue formation in scaffold-free systems. *Nat Mater* **16**, 864, 2017.

Address correspondence to:  
 Kyriacos A. Athanasiou, PhD, PE  
 Department of Biomedical Engineering  
 Henry Samueli School of Engineering  
 University of California, Irvine  
 3418 Engineering Hall  
 Irvine, CA 92697

E-mail: athens@uci.edu

Received: October 4, 2017

Accepted: February 9, 2018

Online Publication Date: March 28, 2018